A 160 GHZ POLARIMETRIC COMPACT RANGE FOR SCALE MODEL RCS MEASUREMENTS

M. J. Coulombe, T. Horgan, and J. Waldman
University of Massachusetts Lowell
Submillimeter-Wave Technology Laboratory
Lowell, MA 01854

J. Neilson, S. Carter, and W. Nixon
U.S. Army National Ground Intelligence Center
Charlottesville VA 22902

ABSTRACT

A fully-polarimetric compact range operating at 160 GHz has been developed for obtaining X-band RCS measurements on 1:16th scale model targets. The transceiver consists of a fast switching, stepped, CW, X-band synthesizer driving dual X16 transmit multiplier chains and dual X16 local oscillator multiplier chains. The system alternately transmits horizontal (H) and vertical (V) radiation while simultaneously receiving H and V. Software range-gating is used to reject unwanted spurious responses in the compact range. A flat disk and a rotating circular dihedral are used for polarimetric as well as RCS calibration. Cross-pol rejection ratios of better than 40 dB are routinely achieved. The compact range reflector consists of a 60 diameter, CNC machined aluminum mirror fed from the side to produce a clean 20 quiet zone. A description of this 160 GHz compact range along with measurement examples are presented in this paper.

Keywords: Compact Ranges, Scale Modeling, RCS Measurements, Submillimeter-Wave, Instrumentation.

1. INTRODUCTION

As radar technology continues to evolve, the availability of high quality, radar cross section (RCS) data is essential for successful development of radar capabilities such as automatic target recognition (ATR). The kind of data needed for these programs includes high-range-resolution (HRR) target profiles and synthetic aperture radar (SAR) images. Computer predictions and compact range measurements are often used to obtain this data when full-scale measurements are not practical, timely, or affordable. The Submillimeter-Wave Technology Laboratory (STL) at UMass Lowell has developed several compact ranges which specialize in using scaled frequencies to measure carefully scaled targets.

The technique of using scale models and scaled frequencies to study electromagnetic scattering dates back to the 1940s [1] and continues to be important and growing in popularity. The use of submillimeter-wave radiation for scale model measurements was first reported in the late 1970s and early 1980s [2]. These early systems were based on narrow-band, optically pumped, submillimeter lasers which are still the best choice for frequencies above 700 GHz.

STL has refined these early laser-based systems into high-performance, compact ranges [3] capable of modeling the characteristics of most modern radar systems at all the popular frequency bands. The laser-based systems have been augmented with schottky diode sideband generators to provide a wide-band capability at THz frequencies. Scale factors used in these submillimeter systems range from 10:1 through 200:1, with frequencies extending up to 3 THz.

At frequencies below about 700 GHz, a completely solid-state approach using varactor multipliers is used. Here, a fast-switching, stepped CW, X-band source drives a series of cascaded doublers and/or triplers augmented with amplifiers where possible, to produce the desired transmit and LO signals. This solid-state approach offers a low maintenance and compact alternative to the laser-based systems. Currently, systems at 160 GHz and 500 GHz have been developed at STL using this approach.

The 160 GHz compact range is based on a fully polarimetric transceiver based on a dual frequency, X-band, source driving four X16 multiplier chains configured as a dual-channel linear-polarized transmit module and a dual-channel linear-polarized receiver. A custom IF converter/amplifier and DSP I-Q demodulator provide for a very low noise receiver with high phase stability. The system operates in a high resolution, stepped CW mode typically measuring 2048 points over the sweep bandwidth. This high resolution sweep allows the entire measurement chamber to be

resolved in range using software range gating techniques. In this way, spurious scattering from the chamber can be isolated and removed.

In following sections, the details of the 160 GHz transceiver will be presented along with the design of the target positioning system and compact range into which it has been incorporated. In addition, data measured from a complex target simulator will be presented along with computer predictions.

2. COMPACT RANGE

The 160 GHz compact range, shown in figure 1, consists of four major functional components; the transceiver, the collimating antenna reflector, the target and calibration positioner, and the data acquisition system.

The transceiver produces about 10 mW of radiation tunable in precise increments between 155 and 165 GHz. This radiation is coupled out of the transmitter's corrugated conical feedhorn as a ~6° FWHM beam which propagates 250 out to the main compact range antenna mirror. The transmit beam at this point is about 27 in diameter. The radiation is collimated by this reflector and propagates downrange to the target located 400 from the reflector. Backscattered radiation from the target retraces the transmit path to the receive feedhorn which has an identical beam pattern. Here the backscattered signal is down-converted through several stages to the final IF of 50 KHz where a DSP lockin amplifier measures its amplitude and phase. The combined transmit and receive patterns result in a 20, 3 dB diameter quiet zone at the target.
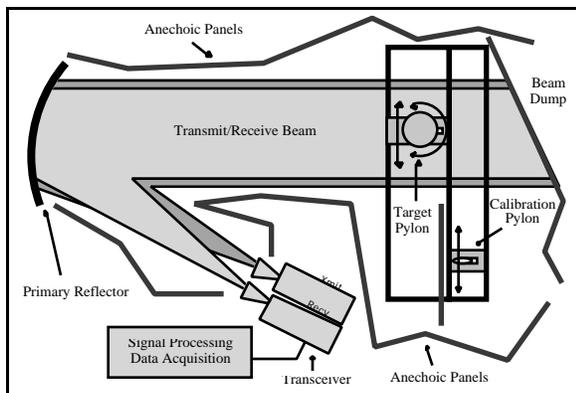

Figure 1. Top View of Compact Range.

The receive feedhorn is typically located adjacent to the transmit feedhorn resulting in a 0.3° bistatic system configuration. Reconfiguration of the system to monostatic operation is achieved with the addition of a 50/50 beam splitter and the rotation of the transmit or receive module by 90°, so that the optic axis of each feedhorn intersects and becomes collinear at the beam splitter.

The compact range antenna is a 60 diameter, 250 focal length, CNC machined, hand polished, aluminum mirror. The mirror edge is rolled to minimize diffracted radiation. The mirror has an optical finish which greatly aids in the alignment of the system as well as testing of the antenna using optical techniques. The mirror is supported on an adjustable mount allowing fine changes in height and orientation.

The target positioner automates the measurement and calibration operations. The positioner allows for the translation of the calibration or target pylons into and out of the beam. The target pylon positions the target in azimuth and elevation. The calibration pylon is used to mount the ogive terminated flat plate and dihedral calibration objects.

The entire compact range chamber is covered with a custom fabricated wedge anechoic material [4] designed at UMass STL and optimized for 160 GHz operation. The anechoic is mounted onto large movable panels which allows the angle of the anechoic to be optimized to reduce backscatter, minimize target-chamber interactions and to deflect unwanted radiation to appropriate areas of the chamber.

All target positioning and transceiver operations are controlled via the Macintosh based data acquisition system. All data acquisition and processing software are written in National Instrument's "Labview"® software which provides a very user-friendly environment without the heavy burdens of learning to program a "C" or "FORTRAN" based graphical user interface. Data processing allows data to be presented as TRCS plots, HRR profiles, and ISAR images.

3. TRANSCEIVER

The transceiver consists of six functional modules; the frequency synthesizer/converter, the transmit multiplier chain, the receive multiplier chain/mixer, the IF converter, the I/Q demodulator, and data acquisition. The system block diagram is presented in figure 2.

The frequency synthesizer/converter module generates three principal frequencies; the transmit multiplier chain drive signal (9.68-10.31 GHz), the receive multiplier chain drive signal (9.49-10.12 GHz), and the IF frequency/phase reference (3 GHz). Because of the X16 multiplication factor, very good spectral purity is extremely important. To achieve these frequencies, the 7.2 GHz synthesizer center frequency is upconverted to the two different X-band drive signals differing in frequency by 187.5 MHz (3.0 GHz/16). This difference,

after X16 multiplication, results ultimately in the 3 GHz IF at the receiver. The 187.5 MHz is also multiplied by X16 to generate a 3 GHz reference which is down-converted in the IF chain along with the horizontal and vertical receive signals.
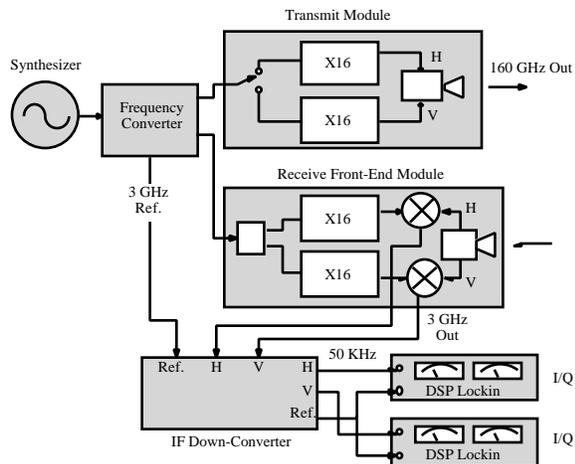

Figure 2. Diagram of 160 GHz Transceiver

The multiplier chains are configured as a transmit module and a receive module as shown in figure 3 along with HeNe alignment lasers and RF enclosures. The transmit multiplier chain consists of a quadrupler amplifier followed by two additional varactor doublers to achieve the desired 160 GHz center frequency. Two identical multiplier chains are used and combined through an orthomode transducer to feed a common corrugated conical feedhorn. Only one chain is normally active at a time, generating greater than 10 mW of output power at either horizontal or vertical polarization. The actual output polarization of the transmitter is slightly elliptical with a linear polarization purity of about 25 dB. In principle, any elliptical polarization state (including circular) is possible by operating both chains simultaneously and carefully controlling the phase and amplitude of each channel. This mode of operation has not yet been demonstrated.

The receiver uses two additional multiplier chains to generate the LOs for the two primary schottky mixers. The received 160 GHz radiation coupled into the receive feedhorn is split in a second orthomode transducer into two schottky mixers and down-converted to a pair of 3 GHz IF signals. The receiver NEP is about 2×10^{-19} W/Hz. The horizontal, vertical and reference 3 GHz IF signals are amplified and further down-converted to 50 KHz. Two Stanford Research SR-850 digital signal processing (DSP) lockin amplifiers (phase-lock demodulators) are used to recover the I&Q signals from the three 50 KHz signals. The DSP technique results in no significant DC offsets or quadrature errors. The I&Q

voltages are then digitized in a 4 channel, 12 bit A-D converter and stored for subsequent processing.
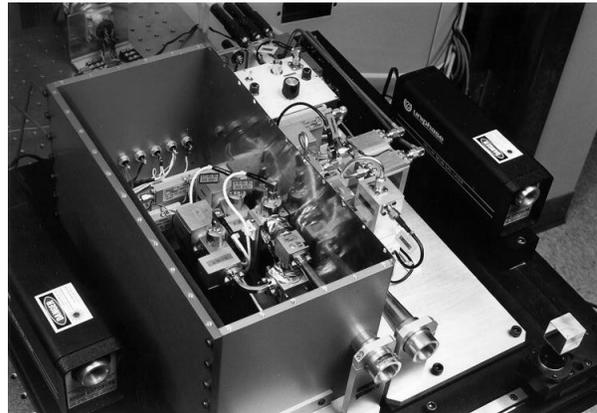

Figure 3. View of Transmit (Left) and Receive (Right) Module with Feed Horns Toward Front.

4. SOFTWARE RANGE GATING

One of the major concerns with any RCS measurement system is the isolation of the target return from unwanted spurious signals. These signals include: leakage in the transceiver, coupling between the feed horns, stray scattering from features in the chamber, or interactions between the target and the chamber. In a pulsed system, signals can be accepted or rejected according to time gates used to activate the receivers only when valid reflections are expected. Unfortunately, narrow time gates introduce significant return losses which are unacceptable when trying to maximize sensitivity with a low power transmitter. In a stepped CW system, a software range gating scheme can be implemented by Fourier transforming the measured complex sweep data from the frequency domain into the time domain. The time gate corresponding to the target is then windowed, removing unwanted chamber responses. Unwanted signals can usually be rejected by better than 40 dB, depending on phase stability and system noise.

Two examples of time domain (range) plots generated with the 160 GHz compact range are illustrated in figure 4. The lower plot shows the range reflections as a function of distance from the zero reference plane with no target in the chamber. The noise floor in these plots is higher than the noise floor of the system due to 40 dB of attenuation applied before the 1st IF mixer to avoid IF saturation for these measurements. This level of noise and dynamic range is typical for the type of targets studied with this system. The typical target range gate is highlighted in gray. Notice all the spurious signals which would interfere with the measurement if software range gating were not used.
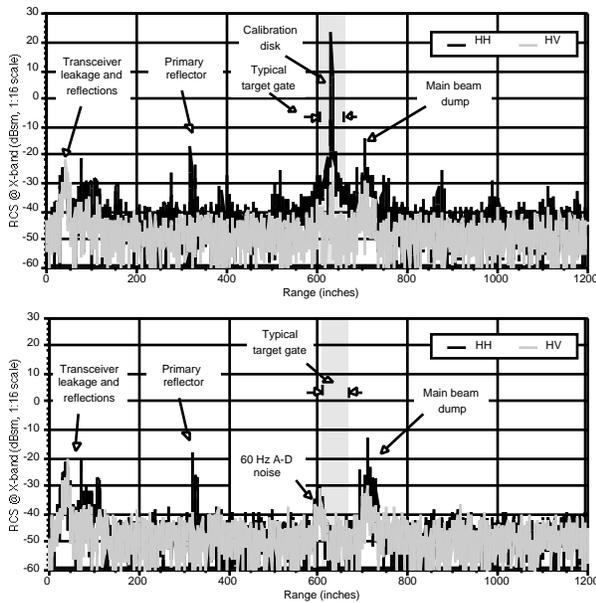
Figure 4. Range Resolved Plots Showing the Entire Compact Range with (Upper) and without (Lower) a Target in the Measurement Chamber.

First, there are a considerable number of spurs coming from the vicinity of transceiver. Since the receiver noise level is 170 dB below the transmit power, it is nearly impossible to shield the receive chain from all flange leaks or diffracted signals from mirrors and misc. structures in the vicinity of the feed horns. The next noticeable scattering comes from the region near the main reflector. Since the beam amplitude profile is nearly gaussian in distribution, a significant amount of power is incident on the edges of the reflector, despite the conservative spot size illumination of the mirror. Some of this energy scatters back to the receive feed horn. Another spurious response is from 60 Hz A-D noise showing up at the front side of the target gate. This spur can be relocated by changing the sweep rate. The last feature is from the beam dump which is a large vertical anechoic panel positioned behind the target and tilted horizontally to deflect stray radiation to the sides of the chamber.

The upper plot in figure 4 illustrates the same measurement sequence, but with a calibration object translated into the beam. A few additional spikes are noticeable in this plot due in part to small measurement errors which manifest themselves as displaced ghosts of the large cal object. Notice the rejection of the cross-pol signal (HV) is ~60 dB below the co-pol (HH) return. This is due in large part to the software polarization calibration scheme described in a later section.

5. CALIBRATION

Calibration is accomplished with a set of objects which are measured sequentially before each run. The calibration objects consist of a flat disk and a dihedral. The cross-sectional area of the calibration objects is chosen to be within 10 to 20 dB of the maximum target RCS anticipated. This allows for a good signal-to-noise ratio and signal-to-clutter ratio for the calibration voltages, producing a clean RCS and polarization calibration. Typically, calibration objects have X-band RCS values of between 10 and 30 dBsm.
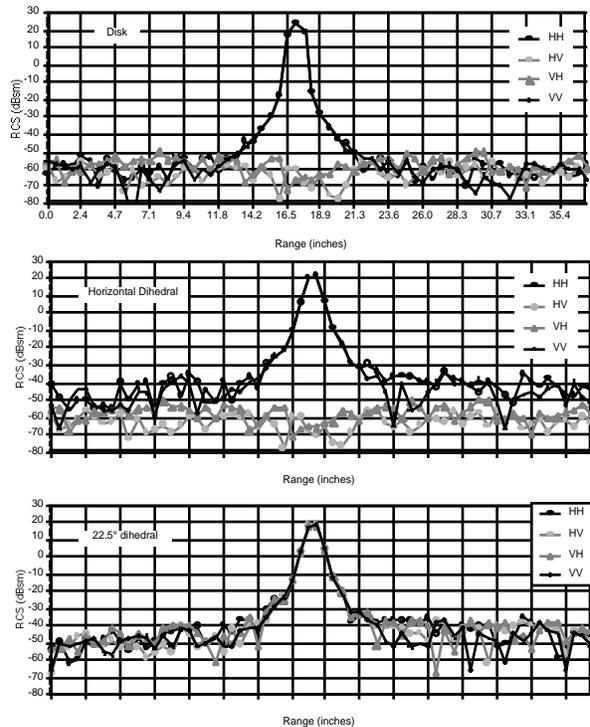

Figure 5. Polarimetric Range Profiles of Three Different Calibration Object Measurements: a Flat Disk (Top) a Horizontal Seam Dihedral (Center), and a 22.5° Seam Dihedral.

A typical calibration sequence consists of the measurement of a flat disk and multiple measurements of a dihedral with its seam oriented at 0° (vertical), 22.5°, 45°, 90° (horizontal), and finally a background measurement (cal object and target pylon translated out of the beam.) A measurement consists of a complete frequency sweep, measuring phase and amplitude at each frequency, for each of the four linear polarization states (HH, HV, VH, VV). The background is subtracted from each of the calibration object measurements and the data is used to calculate the polarization and RCS correction matrix.

Polarization calibration is obtained using a very robust technique described by Chen et al. [5]. Only three measurements are used for the calculation (a disk and

dihedral at 0° and 22.5°). Measurements at other orientations of the dihedral are used only to check the performance of the correction matrices. The cross-pol rejection ratio is improved from between 15 and 25 dB before software calibration to between 40 and 60 dB afterwards. An example of the calibrated flat disk and dihedral and presented in figure 5 showing a very good cross-pol rejection ratio.

6. TARGET POSITIONER

The target positioner, shown with anechoic shielding removed from base in figure 6, is an automated positioning system that serves two major functions: target and calibration object support and orientation, and target and calibration pylon insertion and removal. The basic support for targets and calibration objects is the low-RCS pylon. The pylons consist of a 4' long aluminum pylon with a pointed ogive cross section. The pylon is raked back a minimum of 10° to reduce the radiation back scatter.
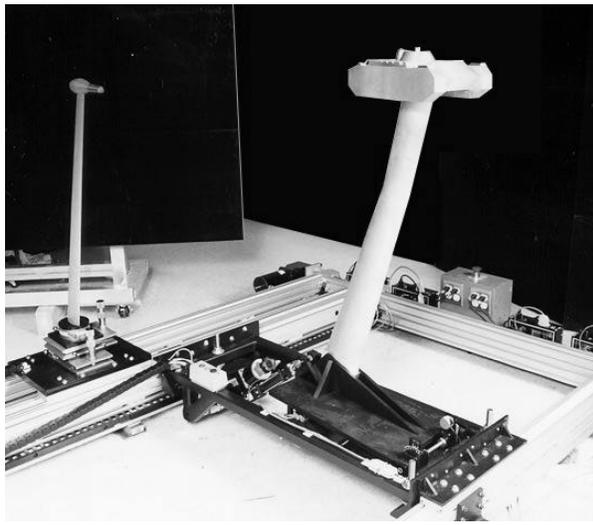

Figure 6. View of the Target Positioning System with Free-Space Calibration Disk (Left) and Complex Target Simulator (Right) Attached to Low-RCS Pylons.

The target pylon is gun-drilled to accept a drive shaft and constant velocity (CV) joint coupled to a mounting flange at the pylon top. This drive shaft is attached to a precision rotary stage at the pylon bottom to provide complete 360° rotation in azimuth. Accurate positioning in azimuth of 0.01° is necessary to allow high quality ISAR imagery to be processed from the measurement data. The entire pylon can be tilted at the base a total of 20°. To achieve a full 80° of travel in elevation, a set of pylon heads biased at -5°, 15°, 35°, and 55° can be interchanged as required to provide from -5° to 80°. A fifth pylon head could be fabricated if elevation angles up to 90° are desired.

When measurements of a target on a groundplane are desired, a special tilting head is retrofitted to the pylon top. This head supports a 40 diameter groundplane which can be tilted to elevation angles usually greater than 10°. Groundplanes with varying roughness and dielectric properties can be used to simulate almost any surface from concrete to sand. Because the ground plane is relatively small, the elevation angles used must be steep enough to allow the image of the target in the groundplane to be visible.

7. MEASUREMENTS

Validation of the range performance as well as the modeling concept is an important part of the normal operation of ranges at STL. This is particularly important in dealing with issues of model fidelity as well as scaling the increasingly-utilized, dielectric materials and absorbers found on full-scale targets. As part of this effort, simple and complex models have been fabricated for the purpose of making measurements which can be compared with full-scale measurements and computer predictions.

The Complex Target Simulator (CTS), shown mounted on a pylon in figure 6, is an example of a complex model developed by the National Ground Intelligence Center (NGIC) and STL as a reference target for microwave and millimeter-wave measurements and computer predictions. This solid metal target has several simple scatterers such as, dihedrals, trihedrals, frustra and a cone-sphere, whose scattering characteristics have been well documented and are easily modeled for computer prediction work.
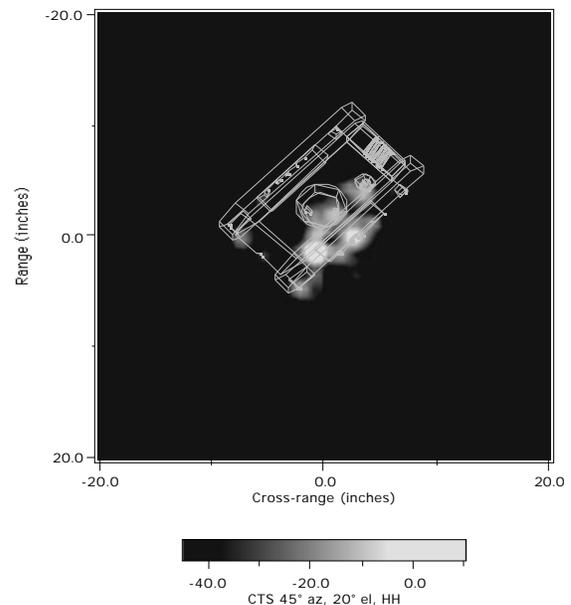

Figure 7. An Example of an X-band ISAR Image of Complex Target Simulator with line drawing overlay (45° az, 20° el, HH).

A geometric model of the simulator was constructed and run on the Xpatch (version 2.1) prediction code. Xpatch is a high-frequency PO/PTD code using shooting and bouncing ray (SBR) techniques. As of 21 June 96, a 10 GHz, monostatic computation of the (full-scale) CTS required 2 minutes of CPU time per "look" on a Silicon Graphics Indigo2 with an R4400 processor. The ray density for this calculation was chosen to be 10 rays per wavelength. The RCS for this target was calculated in 0.25° increments and measured at a 20° elevation angle for direct comparison against a measurement in NGIC's Scale Model Signature Measurements Facility (SSIMFAC).

The CTS was mounted in a "free-space" configuration and measured in the far-field. The azimuth increment was 0.059°. The system bandwidth was set to 10 GHz at a 160 GHz center frequency. This reproduces a 10 GHz center frequency with a 625 MHz bandwidth at full-scale. The transceiver configuration is bistatic at 0.3° and the cross-pol rejection ratio has been measured at >45 dB for this measurement. An ISAR image of the CTS measured in free-space at 45° azimuth and 20° elevation in shown in figure 7.
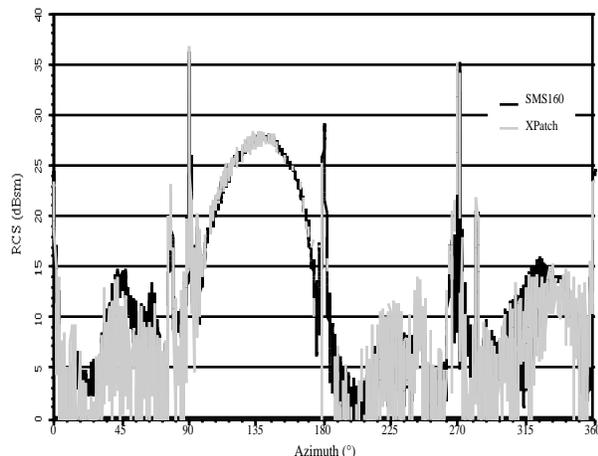

Figure 8. Comparison Between Computer Predictions and Modeled Measurements of the Complex Target Simulator.

A plot comparing the RCS from the Xpatch code and the SSIMFAC measurement of the CTS is presented in figure 8. The SSIMFAC data has been medianized over the measured bandwidth. The Xpatch data was measured at a single frequency and there is a significant amount of scintillation due to the coherent summation from individual scatterers. An analysis of both the Xpatch and SSIMFAC data has allowed identification of a number of major scatterers which have been identified by letter code. Their relative amplitudes and positions are very sensitive to radar line-of-sight. Scatterers A, D and H are trihedral cavity cutouts along the upper right and left sides of the Simulator. Scatterers B, E, F and G are tilted-seam dihedrals that rotate the polarization and are the dominant contributors in the cross-pol channel. The feature indicated by letter C is a large trihedral located on the upper left rear of the Simulator. Comparison overall is very good and the slight differences are under investigation.

8. CONCLUSION

A fully polarimetric compact range based on an X-band source driving X16 multiplier chains to produce radiation at 160 GHz has been described. The system uses software range gating and calibration techniques to achieve a clean target profile with cross-pol rejection ratios of >40 dB. Capabilities for both free-space and ground-plane measurements have been described. A fully automated positioning and calibration system allows unattended range operation 24 hours a day.

The comparison between a computer prediction and scale-model measurement on a relatively complex target was shown to be in good agreement. Because small models are inexpensive to fabricate and since range space requirements are modest, submillimeter compact ranges are proving to be a cost effective, viable complement to full-scale systems and computer codes.

REFERENCES

[1] G. Sinclair, "Theory of Models of Electromagnetic Systems" Proc. IRE, Vol. 36, No. 11, Nov. 1948, pp.1364-1370.

[2] J. Waldman, et al., "Submillimeter Model Measurements and their Application to Millimeter Radar Systems," Fourth Int. Conf. on Infrared and Millimeter Waves and Their Applications, Miami Beach, FL. December 10-15, 1979, pp. 49-50.

[3] M. J. Coulombe et al., "A 585 Ghz Compact Range for Scale Model RCS Measurements" Proc. of the Antenna Measurements and Techniques Association, Dallas TX 1993, pp 129-134

[4] R. H. Giles et al., "Tailoring Artificial Dielectric Materials at Terahertz Frequencies", Proc. of Fourth Int. Symp. of Space THz Technology, Los Angeles, CA, 1993

[5] T.J. Chen et al., "A New Calibration Algorithm of Wide-Band Polarimetric Measurement System", IEEE Trans. of Antennas and Propagation, Vol. 39, No. 8, August 1991

ACKNOWLEDGMENTS